Research Article

Modeling Quantum Well Lasers

Dan Alexandru Anghel, Andreea Rodica Sterian, and Paul E. Sterian

Academic Center for Optical Engineering and Photonics, Faculty of Applied Sciences,
University "Politehnica" of Bucharest, 060042 Bucharest, Romania

Correspondence should be addressed to Andreea Rodica Sterian, andreea_sterian@physics.pub.ro

In semiconductor laser modeling, a good mathematical model gives near-reality results. Three methods of modeling solutions from the rate equations are presented and analyzed. A method based on the rate equations modeled in Simulink to describe quantum well lasers was presented. For different signal types like step function, saw tooth and sinus used as input, a good response of the used equations is obtained. Circuit model resulting from one of the rate equations models is presented and simulated in SPICE. Results show a good modeling behavior. Numerical simulation in MathCad gives satisfactory results for the study of the transitory and dynamic operation at small level of the injection current. The obtained numerical results show the specific limits of each model, according to theoretical analysis. Based on these results, software can be built that integrates circuit simulation and other modeling methods for quantum well lasers to have a tool that model and analysis these devices from all points of view.

1. Introduction

Laser semiconductor diodes are key components in modern optical communications, storage, printing, medicine, and information processing. These types of devices were developed and evolved constantly in the direction of size reduction and integration. A quantum well (QW) laser improves the functioning characteristics of laser diodes in the direction of low threshold current and narrow emission band as well as emitted wavelength dependence on nanostructure dimension (quantum size effect) [1–8].

A quantum well laser is a structure in which the active region of the device is so narrow that quantum confinement occurs, according to quantum mechanics. The wavelength of the light emitted by a quantum well laser is determined by the width of the active region rather than just the band gap of the material from which the device is realized. Consequently, much shorter wavelengths can be obtained from quantum well lasers than from conventional laser

diodes using a particular semiconductor material. The efficiency of a quantum well laser is also greater than a conventional laser diode due to the stepwise form of its density of states function. In the optoelectronic integrated circuits (OEICs), the quantum well lasers will interact optically and electrically with other devices as integrated modulators, optical fibers and coherent amplifiers, detectors, and optical integrated guides [9–19]. A fully analytical method to describe these kind of complex systems cannot be realistic without questionable simplifying assumptions so that the implementations of refined mathematical methods and algorithms as well as circuit simulators become essentially in the applications development [20–24].

2. General Modeling Methods and Techniques

This paper aims at presenting and analyzing modeling techniques for quantum well lasers starting from the rate equations. The issue of modeling of quantum well semiconductor lasers has been addressed by several authors [1–3, 7, 13]. In operation of a laser, effects are involved that can impact a variety of performance parameters of the device. In some cases is crucial to obtain a clear picture of how a laser works in various conditions or parameters. A good laser model which allows calculation and testing of certain parameters of the device is an important result. The main models of laser with quantum wells are based on the description of the semiconductor lasers using the rate equations formalism.

While the first models were based on one pair of equations to describe the density of photons and carriers in the active region, recent approaches include additional rate equations, to take into account, and carriers transport between active region and adjacent layers of the structure.

Note that in most cases the rate equations lead to multiple solutions, although only one solution is correct. Javro and Kang [25] showed that incorrect solutions or without physical sense can be eliminated or avoided through a change of variables in the rate equations.

However, the transformations used are available under certain conditions and for some cases give unrealistic solutions. These shortcomings are caused mainly due to the linear character of the gain-saturation coefficient. More general expression of the gain-saturation coefficient, proposed by Channin can be used to obtain models for operation regimes having a unique solution. Agrawal suggests another expression for this coefficient, which is also suitable. As it is shown, any of these two forms of the gain-saturation coefficient can be used to obtain models with a solution unique of the operation regime.

In this paper, based on known rate equations models we try, firstly, the circuit simulation for two different modeling systems: Simulink and SPICE. The Simulink modeling technique is very simple. It is based on standard rate equations with the sets of parameters given directly in Simulink. The second model is based on the standard rate equations that use a nonlinear gain-saturation term proposed by Channin. In this second model we also describe the circuit level in SPICE with simulation results.

A numerical experiment in MathCad which gives satisfactory results for the study of the transitory and dynamic operation at small level of the injection signal is shortly presented, also.

3. The Model with Linear Gain Saturation, in Simulink

One of the prevailing laser diode models is based on a set of rate equations. The rigorous derivation of these equations originates from Maxwell equations with a quantum mechanical
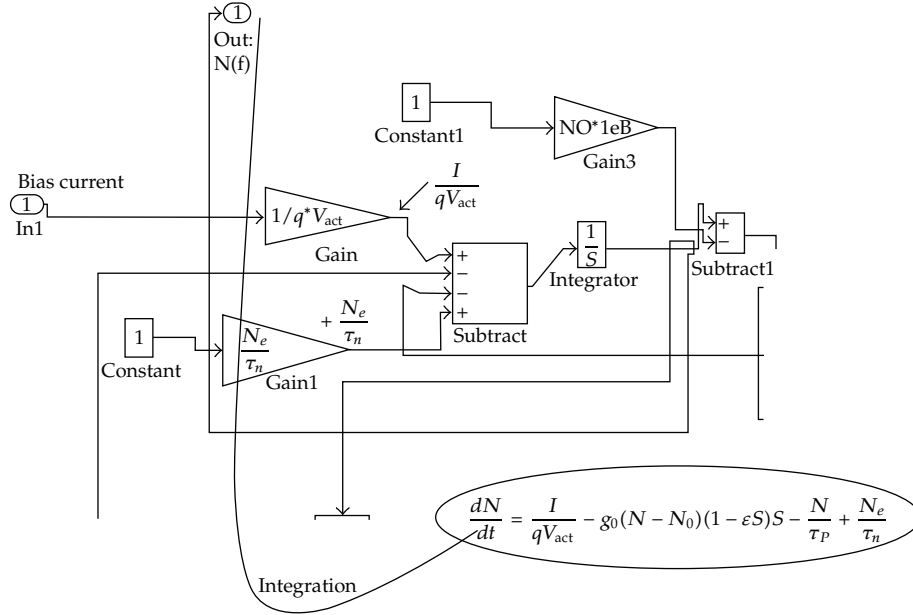
Figure 1: Construction of rate equation block.

approach for the induced polarization. However, the rate equation could also be derived by considering physical phenomena [1, 3, 5]:

$$\frac{dN}{dt} = \frac{I}{qV_{\text{act}}} - g_0(N - N_0)(1 - \varepsilon S)S - \frac{N}{\tau_p} + \frac{N_e}{\tau_n}, \tag{3.1}$$

$$\frac{dS}{dt} = \Gamma g_0(N - N_0)(1 - \varepsilon S)S + \frac{\Gamma \beta N}{\tau_n} - \frac{S}{\tau_p}, \tag{3.2}$$

$$\frac{S}{P_f} = \frac{\Gamma \tau_p \lambda_0}{V_{\text{act}} \eta h c} = \vartheta. \tag{3.3}$$

Equation (3.1) relates the rate of change in carrier concentration N to the injection current I, the carrier recombination rate and the stimulated emission rate. Equation (3.2) relates the rate of change in photon density S to the photons loss, the rate of coupled recombination into the lasing mode, and the stimulated emission rate. The ratio between photon density S to the output power P_f is described in (3.3). The other parameters used have well-known significance [2]. This simple model can be directly implemented with Simulink without any problems.

A direct implementation looks like that in Figure 1.

Figures 1 and 2 show how the rate equations model is constructed in Simulink. with I as input parameter from a signal generator and S, N, and P_f as output parameters. All the parameters in the rate equations can be modified before the simulation starts.

For the simulation we used the following parameters found in specialized papers [1–5]: $\lambda_0 = 1.502 \times 10^{-4}$ cm (laser wavelength), $V_{\text{act}} = 9 \times 10^{-11}$ cm^3 (active region volume),
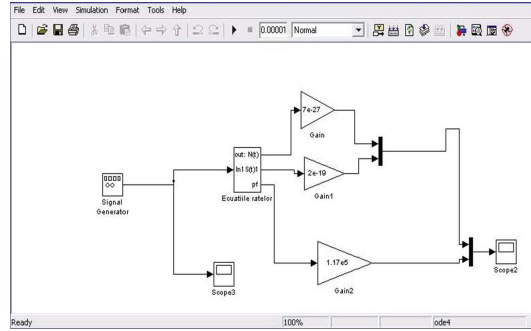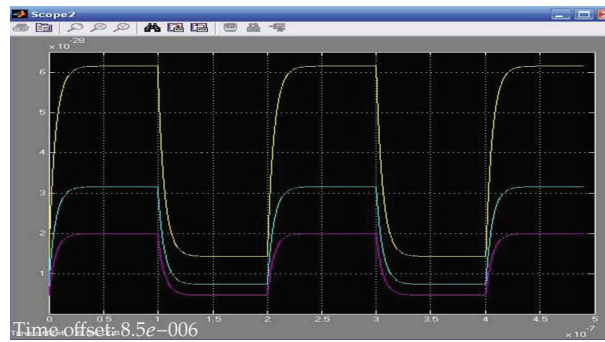
Figure 2: Rate equation in Simulink.

Figure 3: Output for step input signal of 10 mA amplitude and frequency of 5 MHz.
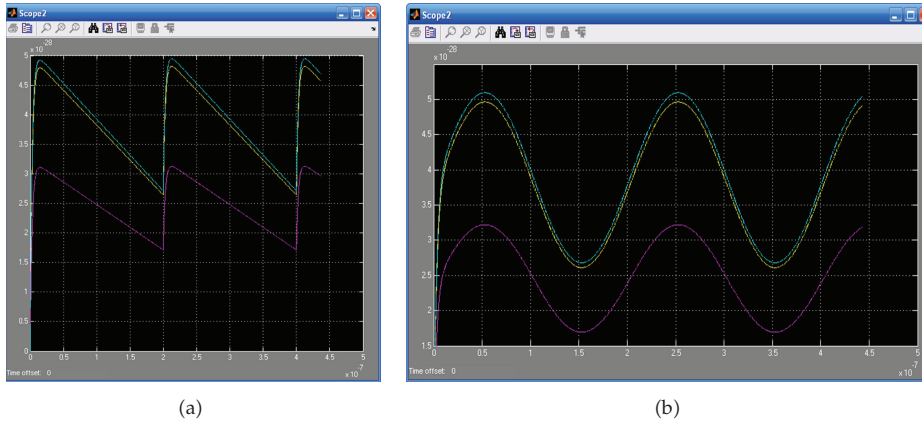

(a)

(b)

Figure 4: Output for saw tooth input signal of 10 mA amplitude and frequency of 5 MHz (a) and for sinusoidal input signal (b).

$\Gamma = 0.44$ (optical confinement factor), $B = 4 \times 10^{-4}$ (spontaneous emission factor), $g_0 = 3 \times 10^{-6}$ cm^3/s (gain coefficient), $N_0 = 1.2 \times 10^{18}$ cm^{-3} (optical transparency density), $\tau_n = 3$ ns (carrier lifetime), $\tau_p = 1$ ps (photon lifetime), $\eta = 0.1$ (quantum efficiency), $N_e = 5.41 \times 10^{10}$ cm^{-3} (equilibrium carrier density), and $\varepsilon = 3.4 \times 10^{-17}$ cm^3 (gain saturation factor).

With the above model different signal forms can be used as input for the quantum well laser. They show that theoretical response of the equations is good in comparison with real results that are obtained in applications. Signals like step function, saw tooth, and sine types are used as input. The results are shown in Figures 3 and 4, which illustrate a very fast response at low current level. Low threshold current is the main feature of quantum well lasers, and it is directly shown for the basic form of rate equations. The simulation is not perfect, and this is because of negative solutions for N and S and high power solution of the equations.

4. The Model with Nonlinear Gain Saturation, in SPICE

To obtain nonnegative solutions for the photon density and the density of carriers in terms of a nonnegative current injection, a different version of the standard rate equations must be formulated. In the corresponding generalized equations (3.1) and (3.2), the linear gain-saturation term is replaced by a nonlinear term proposed by Channin or Agrawal as follows [1–3]:

$$\frac{dN}{dt} = \frac{\eta_i I}{q N_w V_{\text{act}}} - R_w(N) - \Gamma_c v_{\text{gr}} \frac{\alpha(N)}{\Phi(S)} S, \tag{4.1}$$

$$\frac{dS}{dt} = -\frac{S}{\tau_p} + N_w R_{w\beta}(N) + N_w \Gamma_c v_{\text{gr}} \frac{\alpha(N)}{\Phi(S)} S, \tag{4.2}$$

$$\frac{S}{P_f} = \frac{\lambda \tau_p}{\eta_c V_{\text{act}} hc} = \vartheta. \tag{4.3}$$

Equation (4.1) describes the carrier concentration rate dependence on the injection current, the carrier recombination rate $R_w(N)$ and the stimulated emission rate. To take into account all mechanisms of recombination, we consider: $R_w(N) = AN + BN^2 + CN^3$, where A, B, and C are, respectively, the unimolecular, radiative, and Auger recombination coefficients.

Equation (4.2) shows the photon density rate dependence on photon loss, the rate of coupled recombination into the lasing mode, and the stimulated emission rate. Equation (4.3) relates the output power P_f to the photon density S. The other parameters used have well-known significance [2]. In (4.1) and (4.2), the correlation between the material gain and the carrier density is given by the logarithmic carrier-dependent gain term:

$$\alpha(N) = G_0 \ln\left(\frac{R_w(N)}{R_w(N_0)}\right), \tag{4.4}$$

where G_0 is the one quantum well gain coefficient and N_0 is the optical transparency density while the gain-saturation function can take on one of the following two forms:

$$\phi^{-1}(S) = \frac{1}{1 + \varepsilon \Gamma_c S} \text{ (Channin)} \quad \text{or} \quad \phi^{-1}(S) = \frac{1}{\sqrt{1 + \varepsilon \Gamma_c S}} \text{ (Agrawal).} \tag{4.5}$$

An equivalent circuit model based on (4.1)–(4.3) can be implemented in SPICE as in Figure 5. Unlike models based on the rate equations that use a linear gain-saturation term, this circuit model is applicable for all nonnegative values of injection current.
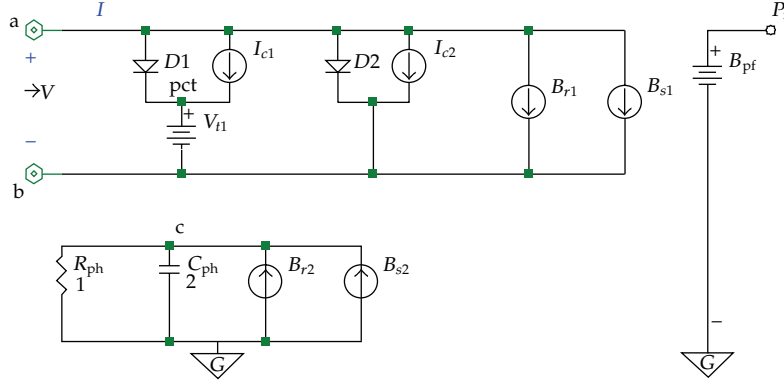
Figure 5: The circuit implementation of the model.

Figure 6 shows the circuit implementation of the model, using suitable variables transformations [25]: $N = N_e \exp(qV/nkT)$ and $P_f = (m + \delta)^2$, which impose nonnegative solutions for N and P_f. The linear recombination and charge storage in the device are described by diodes $D1$ and $D2$ and current sources I_{c1} and I_{c2}. The effects of additional recombination mechanisms and stimulated emission, respectively, on the carrier density are modeled by B_{r1} and B_{s1}, according to (4.11) and (4.13).

The effects of spontaneous and stimulated emission, respectively, are accounted in the circuit by B_{r2} and B_{s2} while R_{ph} and C_{ph} completes the model for the time variation of the photon density. The voltage B_{pf} describe the optical output power of the laser.

The equations for the elements of the circuit in Figure 8 according to [2] are as follows: $I = I_{T1} + I_{D1} + I_{C1} + B_{r1} + B_{s1}$, where

$$I_{T1} = I_{D1} + I_{C1}, \tag{4.6}$$

$$2\tau_p \frac{dm}{dt} + m = B_{r2} + B_{s2}, \qquad B_{pf} = (m + \delta)^2, \tag{4.7}$$

$$I_{D1} = \frac{q N_w V_{act} N_e}{2\eta_i \tau_n} \left[\exp\left(\frac{qV}{nkT} \right) - 1 \right], \tag{4.8}$$

$$I_{D2} = \frac{q N_w V_{act} N_e}{2\eta_i \tau_n} \left[\exp\left(\frac{qV}{nkT} \right) - 1 + \frac{2q\tau_p}{nkT} \exp\left(\frac{qV}{nkT} \right) \frac{dV}{dt} \right], \tag{4.9}$$
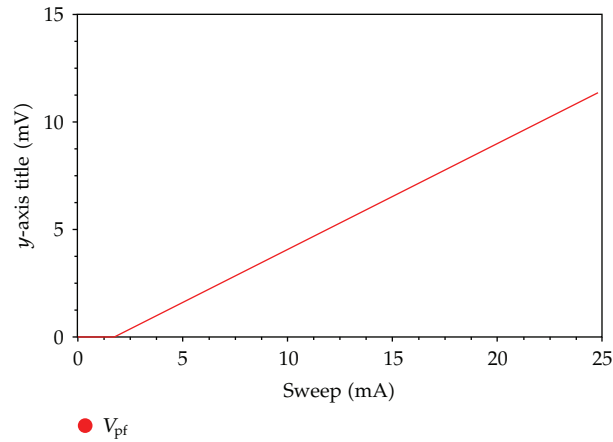
$$I_{c1} = I_{c2} = \frac{q N_w V_{act} N_e}{2\eta_i \tau_n}, \tag{4.10}$$

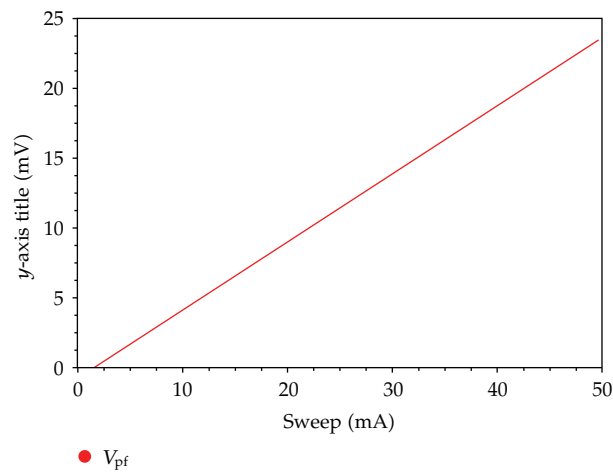$$B_{r1} = \frac{q N_w V_{act}}{\eta_i} R_{\omega 2}(\Theta I_{T1}), \tag{4.11}$$

$$B_{s1} = \frac{\lambda \tau_p N_w \Gamma_c \upsilon_{gr}}{\eta i \eta_c hc} \frac{\alpha(\Theta I_{T1})}{\phi\left(\vartheta(m + \delta)^2 \right)} \vartheta(m + \delta)^2, \tag{4.12}$$

$$B_{r2} = \frac{N_w \eta_c V_{act} hc}{\lambda \vartheta(m + \delta)} R_{\omega 2}(\Theta I_{T1}), \tag{4.13}$$

$$B_{s2} = \tau_p N_w \Gamma_c \upsilon_{gr} \frac{\alpha(\Theta I_{T1})}{\phi\left(\vartheta(m + \delta)^2 \right)} (m + \delta) - \delta. \tag{4.14}$$

(a)

(b)

Figure 6: Answer of optical power with variation of the input bias current between 0 and 25 mA (a) and between 0 and 50 mA (b).

The SPICE netlist was implemented in AIM-SPICE. Calculating the parameters in the netlist is time consuming, and if a calculation is wrong, the netlist will fail in SPICE or the result will not be good. Figures 6, 7, and 8 resulting from simulation with simple DC sweep and transitory sweep illustrate the following:

(i) answer of optical power with variation of the input bias current between 0 and 25 mA (a) and between 0 and 50 mA (b) (Figure 6);

(ii) transient output power in response between 0 and 100 ps (Figure 7);

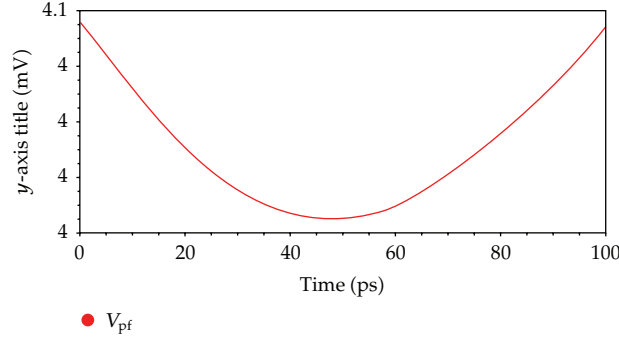(iii) transient output power in response between 0 and 5 ns (Figure 8).

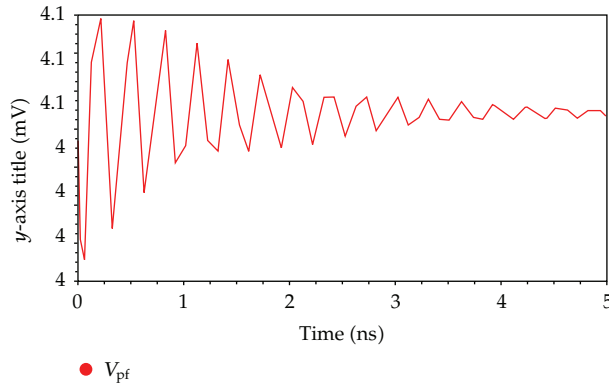**Figure 7:** Transient output power in response between 0 and 100 ps.

Figure 8: Transient output power in response between 0 and 5 ns. Note: Output power is in V because SPICE cannot output variables in W.

5. Numerical Experiment in MathCad

Study of functional characteristics of QWL is possible based on the models described previosly, by implementing MathCad programs to integrate these equations using appropriate algorithms corresponding to different types of pumping signals.

The model given by the equations with linear gain-saturation term (3.1)–(3.3) was integrated for a constant current injection $I_i = 0.05$ A. The waveforms corresponding to I_i and to output optical power P are obtained [13].

The model given by the equations with nonlinear gain saturation (4.1)–(4.3) was integrated for a constant current injection $I_i(t) = 0.025$ A (Figure 9), sinus current injection (Figure 10):

$$I_i(t) = 1 + \sin\left(5 \cdot 10^8 t\right), \tag{5.1}$$

and rectangular current injection (Figure 11), which for several periods can be written as:

$$I_i(t) = 10^{-8} + 0.01 + 0.25 I_i\left(t - 2 \cdot 10^{-9}\right)$$
$$+ 0.25 I_i\left(t - 7 \cdot 10^{-9}\right) + 0.25 I_i\left(t - 12 \cdot 10^{-9}\right). \tag{5.2}$$
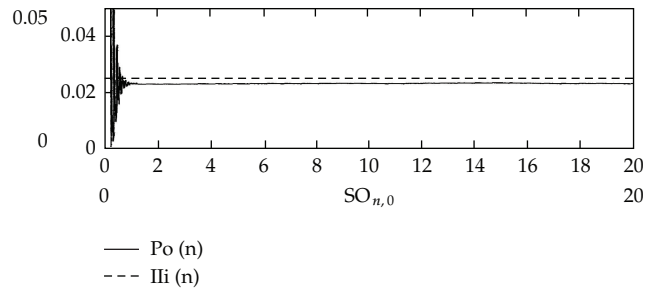
Figure 9: The waveforms corresponding to I_i and to output optical power P.
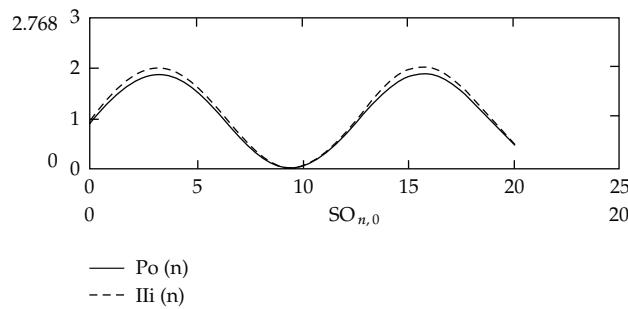

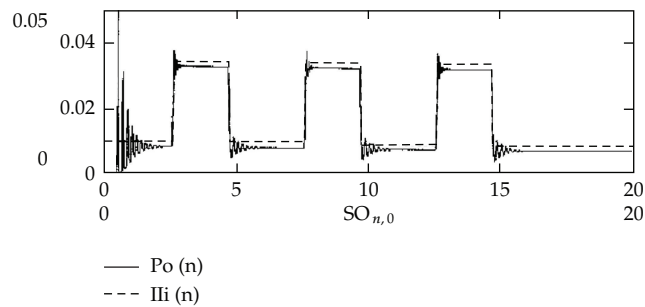Figure 10: The waveforms corresponding to I_i and to output optical power P.

Figure 11: The waveforms corresponding to I_i and to output optical power P.

Simulations results for these large-signal models have shown excellent agreement with experimental data. A corresponding small-signal model has been derived for the quantum well lasers, to study the modulation properties in the frequency domain [13].

6. Conclusions

(1) In the paper, some modeling methods and techniques for the quantum well lasers have been implemented and validated. A suitable modeling technique is very important for technology designing and analyzing of the integrated optoelectronic circuits.

(2) A method based on the rate equations for using Simulink to describe quantum well lasers was presented. For different signal types like step function, saw tooth, and sinus used as input, the results show a good theoretical response of the equations in comparison with the real results obtained in applications. This method is useful to determine the various regions of operation of the laser diode also.

(3) The SPICE simulation of the circuits shows that modifying one parameter will result in new calculations and new SPICE netlist, which is a rather complicated procedure. Simulation is not limited to SPICE; any all-purpose circuit simulator can be used to get similar results.

(4) Generally, all studied models give satisfactory results for the study of the transitory and dynamic operation at small level of the injection signals. At large injection signal levels the obtained numerical results show the specific limits of each model, according to theoretical analysis.

(5) As a future development, software can be built that integrates circuit simulations and other modeling methods for quantum well lasers to have a tool that models these devices from all points of view.

Acknowledgments

References

[1] P. S. Zory, *Quantum Well Lasers*, Academic Press, 1993.

[2] P. V. Mena, S.-M. Kang, and T. A. DeTemple, "Rate-equation-based laser models with a single solution regime," *Journal of Lightwave Technology*, vol. 15, no. 4, pp. 717–729, 1997.

[3] D. S. Gao, S. M. Kang, R. P. Bryan, and J. J. Coleman, "Modeling of quantum-well lasers for computer-aided analysis of optoelectronic integrated circuits," *IEEE Journal of Quantum Electronics*, vol. 26, no. 7, pp. 1206–1216, 1990.

[4] S. Ghoniemy, L. MacEachern, and S. Mahmoud, "Extended robust semiconductor laser modeling for analog optical link simulations," *IEEE Journal on Selected Topics in Quantum Electronics*, vol. 9, no. 3, pp. 872–878, 2003.

[5] M. Dehghan and P. Derakhshan-Barjoei, "A novel dynamic analysus and simulation for quantum-well distributed feedback laser," *Progress In Electromagnetics Research B*, vol. 3, pp. 105–114, 2008.

[6] G. P. Agrawal, *Fiber-Optic Communication Systems*, John Wiley and Sons, New York, NY, USA, 1997.

[7] B. P. C. Tsou and D. L. Pulfrey, "A versatile SPICE model for quantum-well lasers," *IEEE Journal of Quantum Electronics*, vol. 33, no. 2, pp. 246–254, 1997.

[8] N. Bewtra, D. A. Suda, G. L. Tan, F. Chatenoud, and J. M. Xu, "Modeling of quantum-well lasers with electro-opto-thermal interaction," *IEEE Journal on Selected Topics in Quantum Electronics*, vol. 1, no. 2, pp. 331–340, 1995.

[9] A. R. Sterian, "Coherent radiation generation and amplification in erbium doped systems," in *Advances in Optical Amplifiers*, P. Urquhart, Ed., InTech, Vienna, Austria, 2011.

[10] A. R. Sterian, *Amplificatoare Optice*, Editura Printech, Bucureşti, Romania, 2006.

[11] G. Mattioli, M. Scalia, and C. Cattani, "Analysis of large-amplitude pulses in short time intervals: application to neuron interactions," *Mathematical Problems in Engineering*, vol. 2010, Article ID 895785, 15 pages, 2010.

[12] A. R. Sterian and F. C. Maciuc, "Numerical model of an EDFA based on rate equations," in *the 12th International School on Quantum Electronics Laser Physics and Applications*, vol. 5226 of *Proceedings of SPIE*, pp. 74–78, 2003.

[13] A. R. Sterian, *Laserii in ingineria electrica*, Editura Printech, Bucureşti, Romania, 2003.

[14] E. Ştefănescu, A. R. Sterian, and P. Sterian, "Study on the fermion systems coupled by electric dipol interaction with the free electromagnetic field," in *Advanced Laser Technologies*, vol. 5850 of *Proceedings of SPIE*, pp. 160–165, 2005.

[15] E. Stefanescu, P. Sterian, and A. R. Sterian, "The Lindblad dynamics of a Fermi system in a particle dissipative environment," in *ALT '02 International Conference on Advanced Laser Technologies*, Proceedings of SPIE, pp. 160–168, September 2002.

[16] A. Sterian and V. Ninulescu, "Nonlinear phenomena in erbium-doped lasers," in *the International Conference on Computational Science and Its Applications (ICCSA '05)*, O. Gervasi et al., Ed., vol. 3482 of *Lecture Notes in Computer Science*, pp. 643–650, 2005.

[17] A. D. Petrescu, A. R. Sterian, and P. E. Sterian, "Solitons propagation in optical fibers computer experiments for students training," in *the International Conference on Computational Science and its Applications (ICCSA '07)*, O. Gervasi and M. L. Gavrilova, Eds., vol. 4705 of *Lecture Notes in Computer Science*, pp. 450–461, 2007.

[18] A. R. Sterian, *Mecanica cuantică*, Omnia Univ. S.A.S.T., Braşov, Romania, 2008.

[19] A. R. Sterian, "Computer modeling of the coherent optical amplifier and laser systems," in *the International Conference on Computational Science and its Applications (ICCSA '07)*, vol. 4705 of *Lecture Notes in Computer Science*, pp. 436–449, 2007.

[20] C. H. Lee, T. H. Yoon, and S. Y. Shin, "Period doubling and chaos in a directly modulated laser diode," *Applied Physics Letters*, vol. 46, no. 1, pp. 95–97, 1985.

[21] R. Nagarajan, M. Ishikawa, T. Fukushima, R. S. Geels, and J. E. Bowers, "High speed quantum-well lasers and carrier transport effects," *IEEE Journal of Quantum Electronics*, vol. 28, no. 10, pp. 1990–2008, 1992.

[22] C. Cattani and E. Nosova, "Transversal waves in nonlinear Signorini model," in *the International Conference on Computational Science and Its Applications (ICCSA '08)*, vol. 5072 of *Lecture Notes in Computer Science*, pp. 1181–1190, 2008.

[23] C. Cattani, "Harmonic wavelets towards the solution of nonlinear PDE," *Computers & Mathematics with Applications*, vol. 50, no. 8-9, pp. 1191–1210, 2005.

[24] C. Cattani and I. Bochicchio, "Wavelet analysis of bifurcation in a competition model," in *the 7th International Conference on Computational Science (ICCS '07)*, vol. 4488 of *Lecture Notes in Computer Science*, pp. 990–996, 2007.

[25] S. A. Javro and S. M. Kang, "Transforming Tucker's linearized laser rate equations to a form that has a single solution regime," *Journal of Lightwave Technology*, vol. 13, no. 9, pp. 1899–1904, 1995.